

Exploring channel reservoirs in a frontier area with regional CSEM as fluid indicator

Håkon T. Pedersen* and Mike Hiner, EMGS

Summary

In this paper we explore the West Africa - South America analogue proven by the Jubilee and Zaedyus discoveries in Ghana and French Guiana, respectively. Instead of the Turonian turbidite fan reservoirs, we consider younger unproven deep water channel systems in Foz do Amazonas Basin in Brazil which could be analogous to the Campanian pay found in the Teak field in Ghana. We present a geological overview of the basin together with acquisition details and imaging results of a regional 3D CSEM survey in the area. Using CSEM as a fluid indicator, we calculate the Net Rock Volume (NRV) from a channel-shaped EM anomaly and with conservative parameterization we obtain a P10/P90 ratio of 14.7 and an average NRV of $\sim 23000\text{hm}^3$.

Introduction

In September 2011 Tullow Oil announced a significant oil discovery in the Zaedyus prospect in French Guiana that established the Turonian aged Jubilee play from Ghana, West Africa. Following the Zaedyus discovery, a 2012-2013 drilling program of 4 exploration wells targeting nearby turbidites resulted in disappointing commercial success. We will discuss the potential of the younger channel play in the lower Tertiary and upper Cretaceous in Foz do Amazonas basin rather than the Turonian turbidite fans. Continuing the West Africa/South America analogue, the channel systems could resemble the Campanian pay of the Teak-1 exploration well in Ghana (Kosmos Energy, 2011). First, we will give an overview of the geology providing potential reservoir and trapping mechanisms. Second, we will use results of a regional multi-client 3D CSEM survey as a fluid indicator. Acquired in 2013, the survey is bordering French Guiana towards west within 15km of the last exploration well of the drilling program, GM-ES-5, and within 50km of the Zaedyus discovery. Third, we will use the method introduced by Baltar and Roth (2013) to estimate the Net Rock Volume in a sub-region of the CSEM coverage.

Geological overview

The present day shelf margin region of the Foz do Amazonas Basin has undergone significant modification from mass wasting events and debris flows. The basin provides analogous examples for deep water depositional systems in the underlying Tertiary and Cretaceous sections. Based on seismic observations, the shelf is shaped by the orientation of shallow basement that is interpreted as continental crust from potential field data. The basement

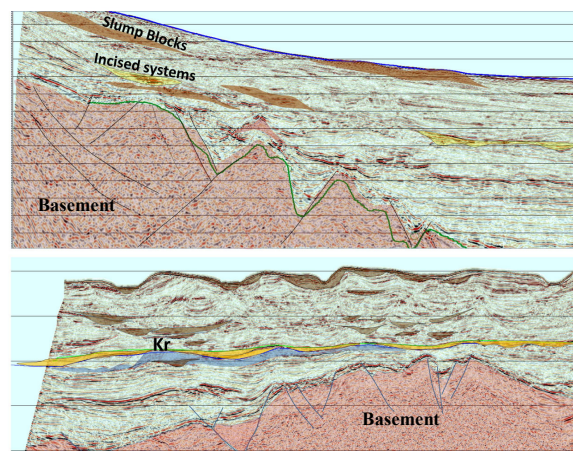


Figure 1: Upper Image: Depositional characteristics of Tertiary and Cretaceous turbidite systems. Lower image: Representative seismic line showing incised canyon systems with stacked channel complexes. The upper Cretaceous is (Kr) is a regional interpretation marking a change in depositional patterns in the basin. Courtesy of Spectrum.

extends outward from the coastline for approximately 130 kilometers before rapidly dropping off in a series of complex fault systems that are related to older rift stage graben systems. The fault blocks in some instances appear to have undergone structural inversion related to the opening of the Atlantic and transpressional deformation related to transfer faults that bound the major basins. The middle Cretaceous section is interpreted regionally to consist of shallow water, lacustrine and fluvial deltaic depositional systems that in-filled Aptian and Albian graben systems during the syn-rift stage of the basin development. Subsequent structural deformation constrained deltaic progradation and developed significant accommodation space along the margin. It is important to note the lateral distance from the present day shelf edge, back to the Cretaceous shelf edge, is approximately 30 kilometers along most of the Foz do Amazonas margin and resulted in primarily aggradational deltaic geometries with relatively steep clinoforms from the shelf edge to the toe of slope. Seismic observations of the shelf edge environment (Figure 1, upper image) indicate potential for over steepened terrains that could develop unstable slope geometries that potentially fail and generate massive debris flows along the slope and toe of slope. The debris flows often contain numerous massive slump blocks in the upper Tertiary section. The slump geometries are less well-defined in the Cretaceous interval due in-part to poor seismic image quality near the shelf edge. In addition to the

Exploring channel reservoirs in Brazil with CSEM

slump geometries, significant deep water channel and canyon systems can be seen. The systems are cut or incised into the sea floor with relief on the canyon walls in some cases exceeding 300 meters. The canyons are often linear, extending from the shelf to the abyssal plain and in some cases running out 80 kilometers on the basin floor before transitioning into unconfined depositional geometries. The upper Tertiary depositional systems provide a reasonable interpretive proxy for turbidite deposition in the lower Tertiary and upper Cretaceous (Figure 1, lower image). Similar canyon and channel systems can be observed to migrate and stack throughout the section, and have similar dimensions to the younger section. Within the objective system stratigraphic traps may develop with lateral and top seals within bends or meanders of incised canyon systems that constrain the turbidite flows. The recent discovery at the Zayedous prospect in French Guiana, approximately 50 kilometers to the northwest suggests that a viable petroleum system exists in the region.

CSEM acquisition and imaging

Approximately 4500km² of 3D CSEM-data were acquired in a 2.5x2.5km receiver grid in water depths ranging from ~200m dropping off the shelf to ~3000m towards North East, Figure 2. The location of the grid was chosen to fill in a 5x5km 2D seismic grid shot by Spectrum. A minimum of 3 azimuth lines were deployed at all times providing true broadside data at 2.5, 5 and 7.5km offset and excellent azimuth data out to ~13km offset for the 0.156Hz base frequency. During CSEM acquisition, receivers are continuously recording while deployed and at times where the source is off or sufficiently far away from a receiver to not cause noise on the magnetotelluric (MT) bandwidth, one can also extract useable MT data. MT data was not included in the imaging results presented in this paper, but a first pass data assessment revealed usable MT periods ranging from ~10 to 1000 seconds, depending on water depth and listening time.

With a 2.5km receiver grid one should expect that smaller hydrocarbon accumulations cannot be resolved. However, considering the frontier nature of the area, early discoveries should be fairly substantial to be commercially viable. There is no linear correlation between receiver distance and sensitivity to volume. Many factors will govern the CSEM sensitivity to a reservoir, most importantly burial depth, area, shape, net pay and resistivity contrast of high vs. low saturation. However, as a rule of thumb, one can expect features wider than the receiver spacing to be sufficient for detection given favourable aforementioned parameters. Due to the size of the survey, the data was divided into 6 subsets, each with 8 receiver lines. The subsets were imaged with 2 overlapping receiver lines to reduce unwanted edge effects due to non-uniform illumination

across subset boundaries. The volumes were later merged into one regional cube. This sequential approach was chosen to a) reduce turn-around time from receiver on deck to inversion product and b) be less computer intensive. To allow for an unbiased study the CSEM results presented are unconstrained, meaning no a-priori information was included (seismic/well logs) nor were resistivity limits applied. The characteristics of this approach become apparent when we compare unconstrained and constrained results from the Xerelete discovery in the Brazilian Campos Basin, Figure 3. An integrated approach provides a sharper resistivity contrast between the background and the anomaly. This allows for an improved interpretation of the anomalous areal extent and consequently reduces the uncertainty in the reserve estimates (Morten et al., 2012). However, it is recommended to always perform an unconstrained study to understand the information content of the CSEM data and get a subsurface image independent of prior interpretations. The latter is particularly important in frontier areas where geological uncertainties are high.

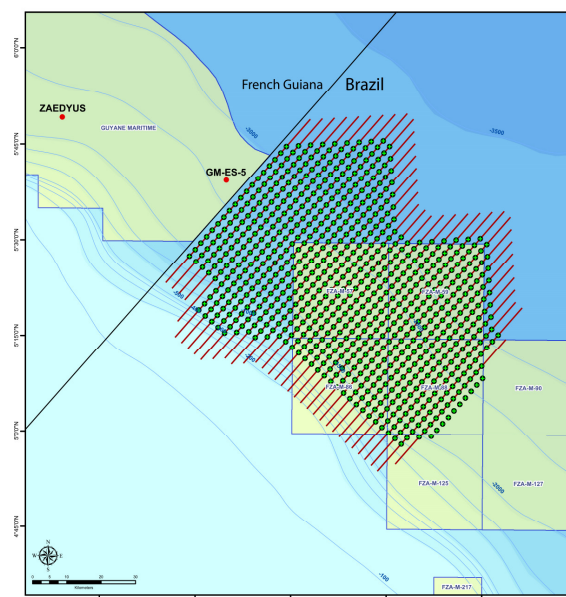


Figure 2: Map view of the CSEM-survey, the French Guiana border and deep water blocks of the 11th Brazilian Licensing Round. Red dots in the Northwest are the Zaedyus discovery and GM-ES-5 well.

The smooth vertical and horizontal resistivity start models used for 3D imaging were populated using less start model dependent anisotropic 2.5D inversions geared towards smooth models through regularization. The main objective of the 2.5D inversions was to capture the resistivity trends of the deep water sediments and not the basement-dominated shelf resistivities.

Exploring channel reservoirs in Brazil with CSEM

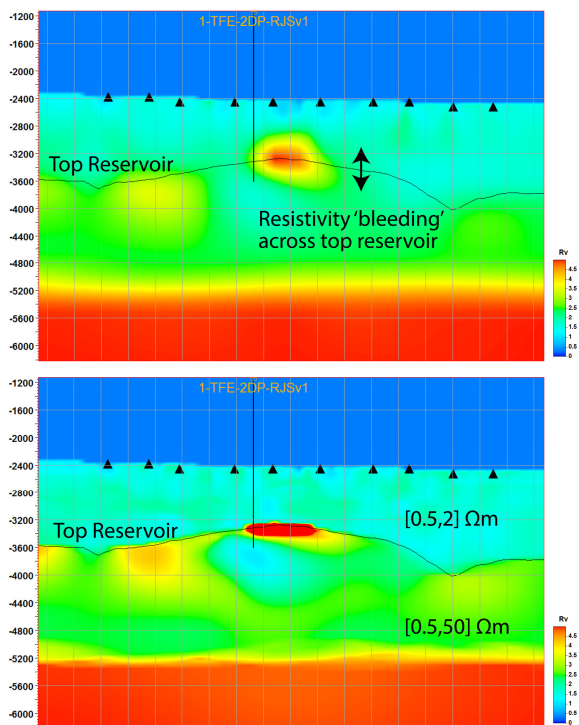


Figure 3: Cross sections along a receiver line displaying the vertical resistivity from anisotropic 3D inversions. The upper image shows unconstrained inversion while the lower image displays results of a constrained inversion with limits applied to the vertical resistivity. Black triangles are receivers and the black line is location of a discovery well.

The data subsets were inverted by the anisotropic 3D inversion described by Zach et al. (2008) and after the *deep water data* are fitted to within the data uncertainty, we stop the inversion process. At this stage there is still an error associated with the shelf area, predominantly caused by too low resistivity due to the basement up-lift. Instead of continuing the inversion where the resistivity will slowly build up and reduce the RMS misfit, we deem this area as uncertain in this first-pass analysis and exclude it from further interpretation. The main drive behind this approach is the understanding that resolving subtle anomalous features from the strong basement response requires additional geophysical data or a joint CSEM-MT study (Hoversten et al., 2013). If we now look at the resistivity cube superimposed on two seismic sections, Figure 4, we clearly see portions which stand out from the background - EM anomalies. From local depth slices we can track the shapes of these anomalies. Next, we generate an attribute map using the vertical resistivity average of a depth window bounded by two copies of the seabed surface. This depth window encompasses the expected burial depths of

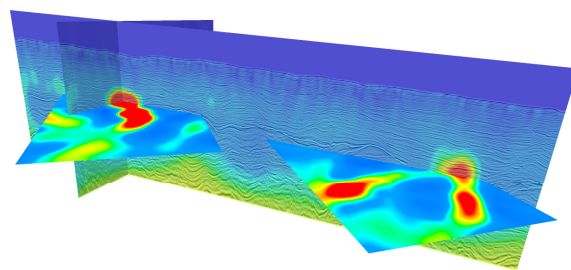


Figure 4: Seismic sections (Courtesy of Spectrum) with superimposed vertical resistivity and depth slices from anisotropic 3D inversion. Warm colours represent high resistivity.

the lower Tertiary and upper Cretaceous channel systems (Figure 5) and the average map is used as input for the reserve estimates.

Reserve estimates

From a sub-region of the regional average resistivity map, we chose an area that included both an EM anomaly and background resistivity values. We focus on channel-shaped EM anomalies with the assumption that these are associated with hydrocarbon saturated sands and calculate the NRV by following the method and notation introduced by Baltar and Roth (2013). The method statistically estimates net pay from the average resistivity by assuming a reservoir resistivity distribution for the anomalous area, following the workflow:

- 1) Calculate the average resistivity over the interval of interest within an anomalous area to obtain a resistivity distribution, R_{CSEM} .
- 2) Choose the background resistivity and anomaly cut-off, R_{bg} and R_{cutoff} , respectively.
- 3) Run a Monte Carlo simulation to calculate the probability distribution for net rock volume.

Previously, we highlighted that anomalies in unconstrained 3D inversions tend to be smeared out both vertically and laterally, increasing the uncertainty of picking appropriate background values. We therefore chose to be on the conservative side for the estimates of R_{bg} and R_{cutoff} . Also, since these channels are not drilled, we do not know what sand resistivity to expect for various hydrocarbon saturations, R . Well logs from Ghana could be included to reduce this range, but that is beyond the scope of this study.

With the fairly conservative parameter choice of $2.1\Omega m < R_{bg} < 2.9\Omega m$, $3.0\Omega m < R_{cutoff} < 3.85\Omega m$ and $15\Omega m < R < 150\Omega m$, we obtain the NRV distribution shown in Figure 6. The average NRV is $\sim 23000\text{hm}^3$ with a P90 and P10 at $\sim 3800\text{hm}^3$ and $\sim 56000\text{hm}^3$, respectively.

Exploring channel reservoirs in Brazil with CSEM

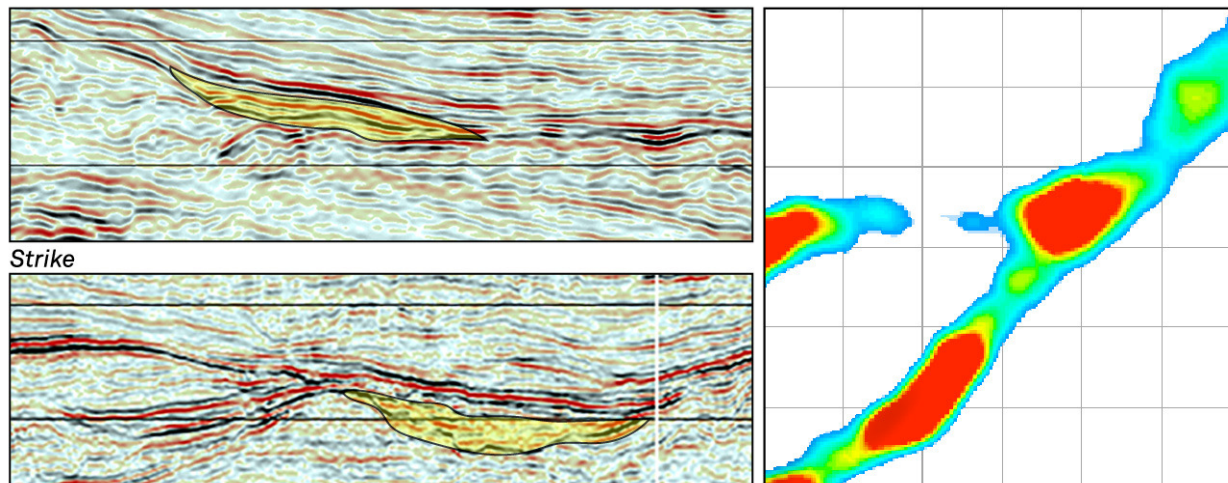


Figure 5: Left images: Seismic lines (Courtesy Spectrum) crossing through a high resistivity incised channel system with no indications of high acoustic impedance. Right image: Average vertical resistivity map from a depth window encompassing the channel depths. Red colour is high average vertical resistivity; low background resistivity is made transparent.

The P10/P90 ratio is 14.7, which according to Rose (2001) falls under an uncertainty range of “Step-out/Extension (5-25)” to “Wildcat in known productive trend (10-120)”. Considering the proximity of the wells in French Guiana to the CSEM survey and the West Africa/South America analogue, one could argue that the results should be classified as the latter while the former is too optimistic.

Conclusion

We have presented a play model which to date has not been drilled in deep water Foz do Amazonas Basin. The proximity to the Zaedyus discovery indicates that there is a working petroleum system and the geological overview provides possible reservoir sands and trapping mechanisms. The regional CSEM results have channel-shaped EM anomalies and we calculated a Net Rock Volume from one of these anomalies. With a fairly conservative parameter choice, we estimated an average NRV of $\sim 23000\text{hm}^3$ and a P10/P90 ratio of 14.7. A risk analysis on the EM anomaly should be performed to exclude potential non-hydrocarbon models (e.g. calcareous turbidites). Assuming such models are deemed improbable as the cause of the anomaly, we expect the P10/P90 ratio to be further reduced by including additional geophysical data in both imaging and reserve estimates.

Acknowledgements

We thank Shengjie Sun for the CSEM imaging results, Daniel Baltar for the NRV estimates, EMGS for permission to present CSEM results and Spectrum for permission to show seismic sections from their multi-client library.

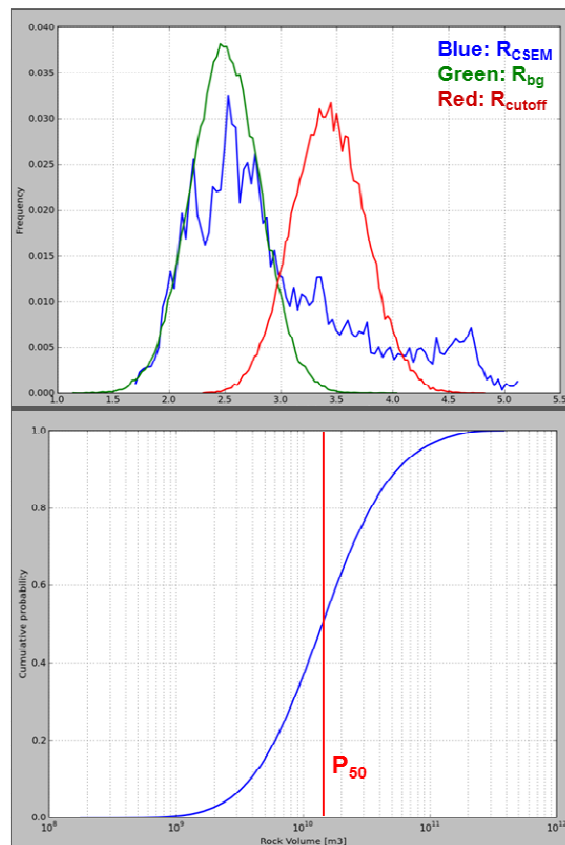


Figure 6: Input to NRV calculations (upper image) with the resulting NRV distribution (lower image).

<http://dx.doi.org/10.1190/segam2014-0825.1>

EDITED REFERENCES

Note: This reference list is a copy-edited version of the reference list submitted by the author. Reference lists for the 2014 SEG Technical Program Expanded Abstracts have been copy edited so that references provided with the online metadata for each paper will achieve a high degree of linking to cited sources that appear on the Web.

REFERENCES

- Baltar, D., and F. Roth, 2013, Reserve estimation methods for prospect evaluation with 3D CSEM data: *First Break*, **31**, 103–111.
- Hoversten, G. M., D. Myer, K. Key, O. Hermann, R. Hobbet, and D. Alumbaugh, 2013, CSEM & MMT base basalt imaging: Presented at the 75th Annual International Conference, EAGE.
- Kosmos Energy, 2011, News release, http://www.kosmosenergy.com/press/kosmos_PR_021011.pdf, accessed 21 March 2014.
- Morten, J. P., F. Roth, S. A. Karlsen, D. Timko, C. Pacurar, P. A. Olsen, A. K. Nguyen, and J. Gjengedal, 2012, Field appraisal and accurate resource estimation from 3D quantitative interpretation of seismic and CSEM data: *The Leading Edge*, **31**, 447–456, <http://dx.doi.org/10.1190/tle31040447.1>.
- Rose, P. R., 2001, Risk analysis and management of petroleum exploration ventures: AAPG.
- Zach, J. J., A. K. Bjørke, T. Støren, and F. Maaø, 2008, 3D inversion of marine CSEM data using a fast finite-difference time-domain forward code and approximate hessian-based optimization: 78th Annual International Meeting, SEG, Expanded Abstracts, **27**, 614–618.